PROCEEDINGS OF SCIENCE

Combining NNLO QCD and NLO EW corrections matched to parton showers for $W^{\pm}Z$ production using MiNNLO$_{\rm PS}$

Silvia Zanoli[a,*]

[a] *Max-Planck-Institut für Physik,*
Föhringer Ring 6, 80805 München, Germany

E-mail: zanoli@mpp.mpg.de

We present results for $W^{\pm}Z$ production at NNLO QCD and NLO electroweak (EW) accuracy matched to parton showers [1]. NNLO QCD corrections matched to parton showers are obtained through the MiNNLO$_{\rm PS}$ method, while NLO EW results matched to parton showers are produced using the POWHEG approach. We identify different combination schemes between QCD and EW corrections with QCD and/or QED showers and we conduct a phenomenological study to analyze their capabilities for describing certain kinematic regions of relevant distributions. We present results for the fully leptonic decay channel $pp \to \ell^+\ell^-\ell'^{\pm}\nu_{\ell'}$, with both $\ell' \neq \ell$ and $\ell' = \ell$, including spin correlation, interferences and off-shell effects. We observe that NNLO QCD corrections with both QCD and QED showers provide an excellent description of the bulk of the cross section, while EW corrections become dominant in the deep tails of kinematic distributions. Our results are in good agreement with recent ATLAS data.

16th International Symposium on Radiative Corrections: Applications of Quantum Field Theory to Phenomenology (RADCOR2023)
28th May - 2nd June, 2023
Crieff, Scotland, UK

*Speaker

PoS(RADCOR2023)068

1. Introduction

Theoretical calculations at the highest accuracy possible in both QCD and electroweak (EW) perturbation theory are essential elements for a proper understanding of current and future LHC data, especially given the increasing level of precision of experimental measurements. As for now, no clear hints of physics beyond the Standard Model (SM) have been observed and precision can serve as a valuable tool for detecting a deviation in the data/theory comparison. In this proceeding, we will review a method to consistently combine next-to-next-to-leading order (NNLO) QCD computations and next-to-leading order (NLO) EW corrections matched to parton showers, as originally presented in [1].

As a case study, we apply this procedure to $W^{\pm}Z$ production, with the vector bosons decaying fully leptonically. This process is particularly interesting because it allows for precise experimental measurements, thanks to the relatively large cross section and clean signature. On the theory side, $W^{\pm}Z$ production represents a convenient framework to test the SM, as it provides direct access to trilinear gauge couplings that are determined by the gauge-symmetry structure of the theory.

2. Outline of the calculation

We consider $W^{\pm}Z$ production with leptonic decays of the vector bosons. Sample diagrams at leading order ($O(\alpha^4)$) are shown in figure 1. The NNLO QCD calculation includes contributions up to $O(\alpha^4\alpha_s^2)$. NNLO corrections are expected to be large (10–15% [2]) since this process is affected by the radiation zero effect at LO [3]. It is important to note that gluon-gluon contributions are not possible because of charge conservation. The NLO EW correction is of order $O(\alpha^5)$. Real corrections are of pure QED type (emissions of photons), while virtual contributions are given by one-loop corrections involving W, Z and Higgs bosons, photons and fermions (including heavy quarks). Photon-induced contributions are not present, while photon-quark contributions have been neglected because of the small photon content in the proton (formally, it is suppressed by an extra power of the coupling α times a collinear logarithm). To reach NNLO QCD and NLO EW accuracy matched to partons showers, we follow three main steps: firstly, we separately generate NNLO QCD and NLO EW accurate results within the Powheg-Box-Res framework [4], as explained in section 2.1. Secondly, we shower the two sets of events through Pythia8 [5] employing a dedicated veto procedure for QCD and QED parton showers. This procedure is described in section 2.2. Thirdly, we combine the QCD and the EW results using appropriate combination schemes at the level of differential distributions, as explained in section 2.3.

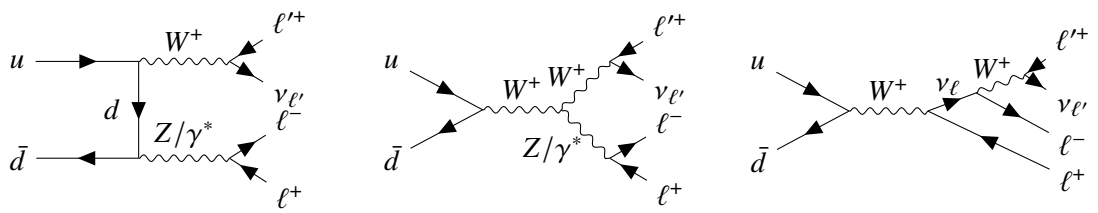

Figure 1: Sample LO diagrams for $pp \to \ell^+\ell^-\ell'^{\pm}\nu_{\ell'}$.

2.1 Generation of events

NNLO QCD results are obtained using the MiNNLO$_{\rm PS}$ method [6, 7]. MiNNLO$_{\rm PS}$ was introduced to consistently match NNLO QCD computations with parton showers, and it relies on the Powheg [8–11] formalism. If we consider the production of a colour singlet F, we can write the fully differential MiNNLO$_{\rm PS}$ cross section starting from a Powheg calculation for F+J, where J represents a light jet, as follows:

$$\mathrm{d}\sigma_{\rm F}^{\rm MiNNLO_{PS}} = \mathrm{d}\Phi_{\rm FJ}\, \bar{B}^{\,\rm MiNNLO_{PS}} \times \left\{ \Delta_{\rm pwg}(\Lambda_{\rm pwg}) + \mathrm{d}\Phi_{\rm rad}\, \Delta_{\rm pwg}(p_{\rm T,rad})\, \frac{R_{\rm FJ}}{B_{\rm FJ}} \right\} . \tag{1}$$

$\Delta_{\rm pwg}$ represents the Powheg Sudakov form factor (with cutoff $\Lambda_{\rm pwg} = 0.89\,\mathrm{GeV}$), $\Phi_{\rm rad}$ and $p_{\rm T,rad}$ are the phase space and transverse momentum of the radiation, and $B_{\rm FJ}$ and $R_{\rm FJ}$ represent the squared tree-level and real matrix elements for FJ production, respectively. The usual Powheg $\bar{B}$ function is modified into $\bar{B}^{\,\rm MiNNLO_{PS}}$ to reach NNLO accuracy. Symbolically, it reads

$$\bar{B}^{\,\rm MiNNLO_{PS}} = e^{-S} \left\{ \frac{\mathrm{d}\sigma_{\rm FJ}^{(1)}}{\mathrm{d}\Phi_{\rm FJ}} \left(1 + S^{(1)}\right) + \frac{\mathrm{d}\sigma_{\rm FJ}^{(2)}}{\mathrm{d}\Phi_{\rm FJ}} + \left(D - D^{(1)} - D^{(2)}\right) \times F^{\rm corr} \right\} , \tag{2}$$

where $\mathrm{d}\sigma_{\rm FJ}^{(1,2)}$ are the LO and NLO differential FJ cross sections, S is an appropriate Sudakov form factor, with $S^{(1)}$ being the $O(\alpha_s)$ term in its expansion, and the last term $(D - D^{(1)} - D^{(2)})$ represents the α_s^3 correction needed to reach NNLO accuracy. This contribution depends only on the transverse momentum $p_{\rm T}$ of the colour singlet F, and it is thus spread on the FJ phase space through a suitable function $F^{\rm corr}$. The D terms are obtained from the following $p_{\rm T}$-resummation formula

$$\mathrm{d}\sigma_{\rm F}^{\rm res} = \frac{\mathrm{d}}{\mathrm{d}p_{\rm T}} \left\{ e^{-S}\mathcal{L} \right\} = e^{-S} \underbrace{\left\{ -S'\mathcal{L} + \mathcal{L}' \right\}}_{\equiv D} , \tag{3}$$

where $\mathcal{L}$ is the luminosity factor up to NNLO. More details on the method can be found in [6, 7].

Our implementation is performed within the Powheg-Box-Res framework. Tree-level and one-loop amplitudes are obtained from OpenLoops [12–14] through the interface developed in [15], while two-loop amplitudes are provided by VVAmp [16, 17] using the interface to Matrix [18] that was developed in [19]. Moreover, in our calculation we also make use of hoppet [20], lhapdf [21] and hplog [22]. The adopted MiNNLO$_{\rm PS}$ settings are described in section 2.2 of the original publication [1]. NLO EW results are obtained through a separate Monte Carlo event generator that is able to compute NLO QCD, NLO EW and NLO QCD+EW calculations for diboson processes. Also in this case, we rely on the Powheg-Box-Res framework and we use OpenLoops as amplitude provider. This implementation is equivalent to the one presented in [23].

Our implementations have been carefully tested against fixed-order computations obtained using Matrix. Validation plots are presented in section 3.2 of the original publication [1].

2.2 Veto procedure

The matching of NNLO QCD and NLO EW computations with QCD and QED parton showers requires a dedicated veto procedure. Our veto procedure is inspired by Appendix D of [24] and it

proceeds as follows: we let the parton-shower provider (Pythia8) generate emissions in the entire kinematically allowed phase space and then we accept or reject the event according to its shower history. More precisely, when dealing with NNLO_{QCD}+PS computations, we need to restrict the QCD emissions generated by the shower, while QED radiation is unconstrained. To this end, we scan all the QCD emissions generated by the shower, we calculate the hardest transverse momentum p_{T}^{max} and we verify that it is smaller than the transverse momentum of the QCD emission generated by Powheg. If this requirement is satisfied, we accept the event, otherwise we try to shower it again. After 1000 unsuccessful attempts, the event is rejected. By contrast, when computing NLO_{EW}+PS results we restrict QED emissions generated by Pythia8, while QCD radiation is unconstrained. In this case, we adopt the multiple-radiation scheme of Powheg (`allrad 1`) [15] through which we can define three different starting scales for the QED shower by generating up to one photon per singular region of the process (namely, up to one photon as initial-state radiation and up to two photons as final-state radiation, one from the W and one from the Z decays). We then check, region by region, whether the emissions generated by Pythia8 have a hardness smaller than the emissions produced by Powheg. Also in this case, after 1000 unsuccessful attempts, the event is rejected.

2.3 Combination of NNLO QCD and NLO EW corrections matched with parton showers

The combination of NNLO_{QCD}+PS and NLO_{EW}+PS results is done a posteriori, at the level of differential distributions. We recall that, at fixed order, QCD and EW higher-order corrections can be combined either in an additive or a multiplicative way [25]. When considering the matching with parton showers, one needs to define a combination scheme of QCD and EW corrections that does not spoil the formal accuracy of the calculation and does not introduce any double counting. We introduce the following notation $(\text{N})\text{NLO}_{\text{X}}^{(\text{Y})_{\text{PS}}}$, with $\text{X} \in \{\text{QCD}, \text{EW}\}$ and $\text{Y} \in \{\text{QCD, QED, QCD and QED}\}$, to refer to the (N)NLO calculation in X perturbation theory matched to Y parton showers. Moreover, we define a generic higher-order correction to the LO computation as $\delta\text{N(N)LO}_{\text{X}}{}^{(\text{Y})_{\text{PS}}} = \text{N(N)LO}_{\text{X}}^{(\text{Y})_{\text{PS}}} - \text{LO}_{\text{X}}^{(\text{Y})_{\text{PS}}}$, and a multiplicative K-factor as $\text{K-N(N)LO}_{\text{X}}^{(\text{Y})_{\text{PS}}} = \text{N(N)LO}_{\text{X}}^{(\text{Y})_{\text{PS}}}/\text{LO}_{\text{X}}^{(\text{Y})_{\text{PS}}}$. The combination of NNLO QCD and NLO EW computations matched to QCD and QED parton showers can thus be obtained through the following schemes:

additive schemes:

$$1.\ \text{NNLO}_{\text{QCD}}^{(\text{QCD,QED})_{\text{PS}}} + \delta\text{NLO}_{\text{EW}}^{(\text{QCD,QED})_{\text{PS}}} = \text{NNLO}_{\text{QCD+EW}}^{(\text{QCD,QED})_{\text{PS}}} \tag{4}$$

$$2.\ \text{NNLO}_{\text{QCD}}^{(\text{QCD,QED})_{\text{PS}}} + \delta\text{NLO}_{\text{EW}}^{(\text{QED})_{\text{PS}}} \tag{5}$$

$$3.\ \text{NLO}_{\text{EW}}^{(\text{QCD,QED})_{\text{PS}}} + \delta\text{NNLO}_{\text{QCD}}^{(\text{QCD})_{\text{PS}}} \tag{6}$$

multiplicative schemes:

$$4.\ \text{NNLO}_{\text{QCD}}^{(\text{QCD,QED})_{\text{PS}}} \times \text{K-NLO}_{\text{EW}}^{(\text{QCD,QED})_{\text{PS}}} = \text{NNLO}_{\text{QCD}\times\text{EW}}^{(\text{QCD,QED})_{\text{PS}}} \tag{7}$$

$$5.\ \text{NNLO}_{\text{QCD}}^{(\text{QCD,QED})_{\text{PS}}} \times \text{K-NLO}_{\text{EW}}^{(\text{QED})_{\text{PS}}} \tag{8}$$

$$6.\ \text{NLO}_{\text{EW}}^{(\text{QCD,QED})_{\text{PS}}} \times \text{K-NNLO}_{\text{QCD}}^{(\text{QCD})_{\text{PS}}} \tag{9}$$

$$7.\ \text{NNLO}_{\text{QCD}}^{(\text{QCD})_{\text{PS}}} \times \text{K-NLO}_{\text{EW}}^{(\text{f.o.})}. \tag{10}$$

These schemes are NNLO QCD and NLO EW accurate, consistently matched to QCD and QED parton showers and differ only for terms beyond accuracy. Schemes number 1 and 4 are our *default*

additive and multiplicative combinations, for which dedicated short-hand notations have been introduced. Note that in (10) the EW K-factor is obtained at fixed order (we use MATRIX+OPENLOOPS).

3. Phenomenological results

In this section we present results for $W^\pm Z$ production at NNLO QCD and NLO EW accuracy matched to parton showers. For the sake of simplicity, we specifically consider the process $pp \to \mu^+\nu_\mu e^+e^-$, but all our conclusions apply to any leptonic decay channel. We consider 13 TeV centre-of-mass energy collisions and we employ the following inputs [26]:

$$G_F = 1.16639 \times 10^{-5}\,\text{GeV}^{-2}\,, \quad m_Z = 91.1876\,\text{GeV}\,, \quad \Gamma_H = 4.07\,\text{MeV}\,,$$
$$m_W = 80.385\,\text{GeV}\,, \quad \Gamma_Z = 2.4952\,\text{GeV}\,, \quad m_t = 173.2\,\text{GeV (on-shell)}\,,$$
$$\Gamma_W = 2.0854\,\text{GeV}\,, \quad m_H = 125\,\text{GeV}\,, \quad \Gamma_t = 1.347878\,\text{GeV}\,.$$

We use the complex-mass scheme [27, 28] and EW parameters are obtained in the G_μ scheme [14]. We use the `NNPDF31_nnlo_as_0118_luxqed` PDFs set [29–31], with $\alpha_s = 0.118$. In the NNLO computation, renormalization and factorization scales are set according to the MINNLO$_{\text{PS}}$ method, while in the NLO EW results we use

$$\mu_{\text{F}} = \mu_{\text{R}} = \frac{1}{2}\left(\sqrt{m^2_{e^+e^-} + p^2_{\text{T},e^+e^-}} + \sqrt{m^2_{\mu\nu_\mu} + p^2_{\text{T},\mu\nu_\mu}}\right)\,, \tag{11}$$

where $m_{e^+e^-}$ and p_{T,e^+e^-} ($m_{\mu\nu_\mu}$ and $p_{\text{T},\mu\nu_\mu}$) represent the invariant mass and the transverse momentum of the Z boson (W boson). Scale uncertainties are obtained using the customary seven-point scale variation. In the combination of QCD and EW results, we correlate the scales. The parton shower provider is PYTHIA8 [5] with the Monash 2013 tune [32]. In this phenomenological analysis, we employ two different setups summarized in table 1. Note that physical leptons are obtained dressing leptons ℓ with photons γ within a distance $\Delta R_{\ell,\gamma} = \sqrt{\Delta\phi^2_{\ell\gamma} + \Delta\eta^2_{\ell\gamma}} < 0.1$.

The left plot of figure 2 shows the invariant mass $m_{e^+e^-}$ of the reconstructed Z boson in the `inclusive setup`. We observe that the pure QCD result (NNLO$^{(\text{QCD})_{\text{PS}}}_{\text{QCD}}$) is not suitable to describe appropriately this observable as it misses important collinear QED effects, as already pointed out in [33–35] for Drell-Yan production. These effects are of order 40% in the low mass region ($m_{e^+e^-} \simeq 70$ GeV). A similar conclusion holds for the NLO$^{(\text{QCD,QED})_{\text{PS}}}_{\text{EW}} + \delta\text{NNLO}^{(\text{QCD})_{\text{PS}}}_{\text{QCD}}$ combination, which misses large QED effects in the NNLO QCD computation. We observe that our default multiplicative and additive results are in very good agreement with both NNLO$^{(\text{QCD,QED})_{\text{PS}}}_{\text{QCD}}$ and NNLO$^{(\text{QCD})_{\text{PS}}}_{\text{QCD}} \times \text{K-NLO}^{(\text{f.o.})}_{\text{EW}}$.

`inclusive setup`
$66\,\text{GeV} < m_{e^+e^-} < 116\,\text{GeV}$

`fiducial setup`
$\lvert m_{e^+e^-} - m_Z\rvert < 10\,\text{GeV}$
$p_{T,e^\pm} > 15\,\text{GeV}, \quad p_{\text{T},\mu} > 20\,\text{GeV},$
$\lvert\eta_\ell\rvert < 2.5, \quad m_{\text{T},W} > 30\,\text{GeV},$
$\Delta R_{e^+e^-} > 0.2, \quad \Delta R_{e^\pm\mu} > 0.3$

Table 1: Definition of `inclusive setup` and `fiducial setup`.

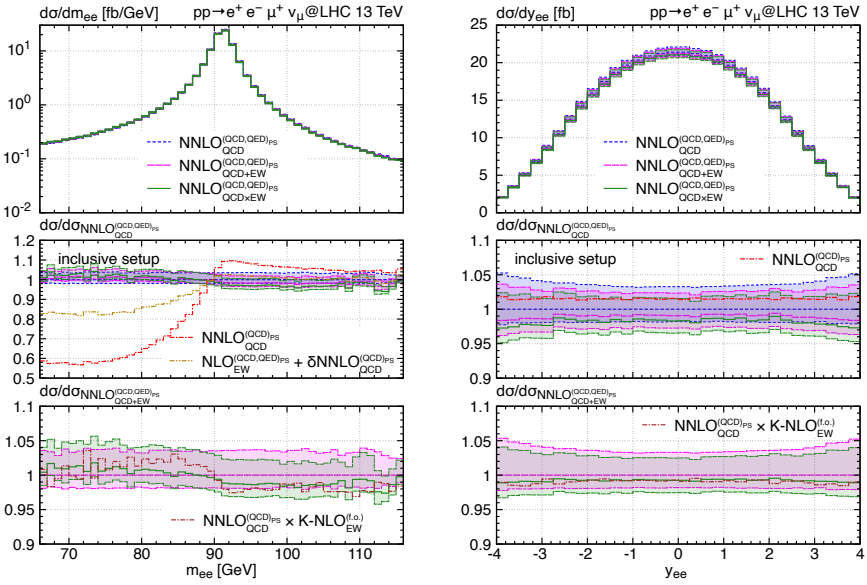

Figure 2: Differential distributions in the Z-boson invariant mass (left) and rapidity (right) for W^+Z production. We adopt the `inclusive setup`.

In the right plot of figure 2 we show the rapidity $y_{e^+e^-}$ of the reconstructed Z boson in the `inclusive setup`. Pure QED effects can be estimated by comparing the $\text{NNLO}_{\text{QCD}}^{(\text{QCD})_{\text{PS}}}$ and $\text{NNLO}_{\text{QCD}}^{(\text{QCD,QED})_{\text{PS}}}$ results, and they turn out to be of order -1–2%. Our default multiplicative and additive schemes are in excellent agreement, and they show effects of pure weak origin of order -2–3%. Notice that the default multiplicative combination is almost perfectly on top of the scheme with a fixed-order EW K-factor ($\text{NNLO}_{\text{QCD}}^{(\text{QCD})_{\text{PS}}} \times \text{K-NLO}_{\text{EW}}^{(\text{f.o.})}$), which means that this observable does not depend on photon emissions beyond the first one.

Figure 3 shows the missing transverse momentum $p_{\text{T,miss}}$ in the `inclusive setup` (left) and in the `fiducial setup` (right). Looking at the deep tail of this distribution, we observe the typical enhancement of EW Sudakov logarithms: in the default multiplicative scheme, EW effects are of order -15% at $p_{\text{T,miss}} \simeq 500$ GeV, while they are of order -4% in the default additive combination in the same $p_{\text{T,miss}}$ region. The discrepancy between these two results can be explained in terms of giant K-factors [25] that arise in configurations where the hard system is given by a vector boson and a jet, leaving the second vector boson soft. Moreover, our default multiplicative prediction shows a smaller EW enhancement when compared to $\text{NNLO}_{\text{QCD}}^{(\text{QCD})_{\text{PS}}} \times \text{K-NLO}_{\text{EW}}^{(\text{f.o.})}$ and $\text{NNLO}_{\text{QCD}}^{(\text{QCD,QED})_{\text{PS}}} \times \text{K-NLO}_{\text{EW}}^{(\text{QED})_{\text{PS}}}$: this behaviour can be explained in terms of giant QCD K-factors which are associated with QCD emissions produced by the shower on top of the NLO EW computation.

In figure 4, we present the invariant mass $m_{3\ell}$ of the three charged leptons in the `inclusive setup` (left) and `fiducial setup` (right). For this observable, we note that EW effects become larger when fiducial cuts are applied. In fact, at invariant-mass values $m_{3\ell} \sim 2$ TeV, they increase from about -10% to about -20–30% when moving from the `inclusive setup` to the `fiducial setup`. This feature can be explained as follows: in the `inclusive setup` the high-$m_{3\ell}$ region

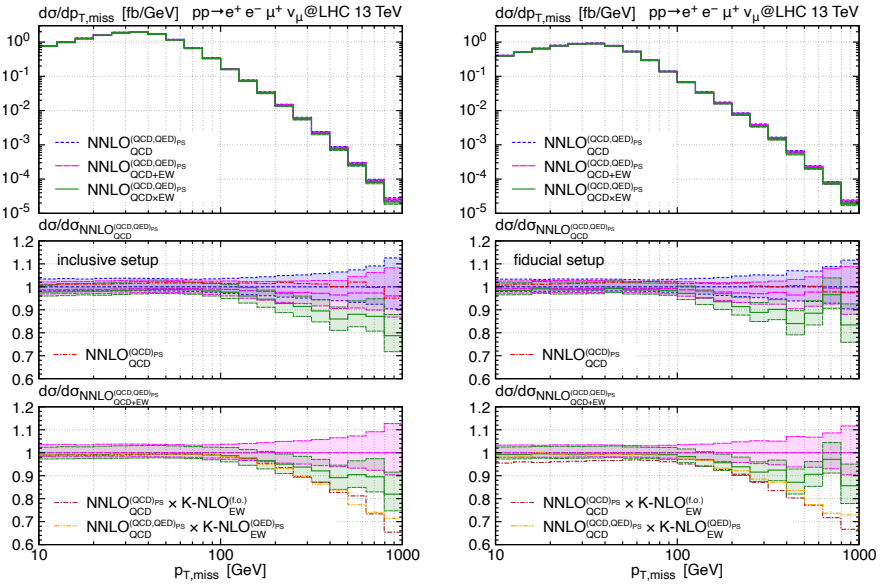

Figure 3: Differential distributions in the missing transverse momentum $p_{\mathrm{T,miss}}$ for W^+Z production. Results are obtained in the `inclusive setup` (left) and the `fiducial setup` (right).

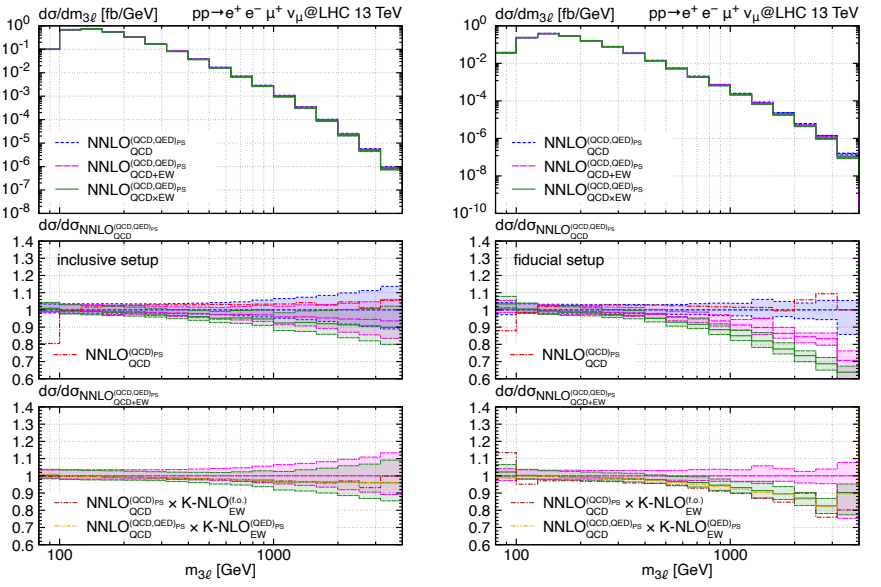

Figure 4: Differential distributions in the invariant mass of the three final-state leptons in W^+Z production. Results are obtained in the `inclusive setup` (left) and the `fiducial setup` (right).

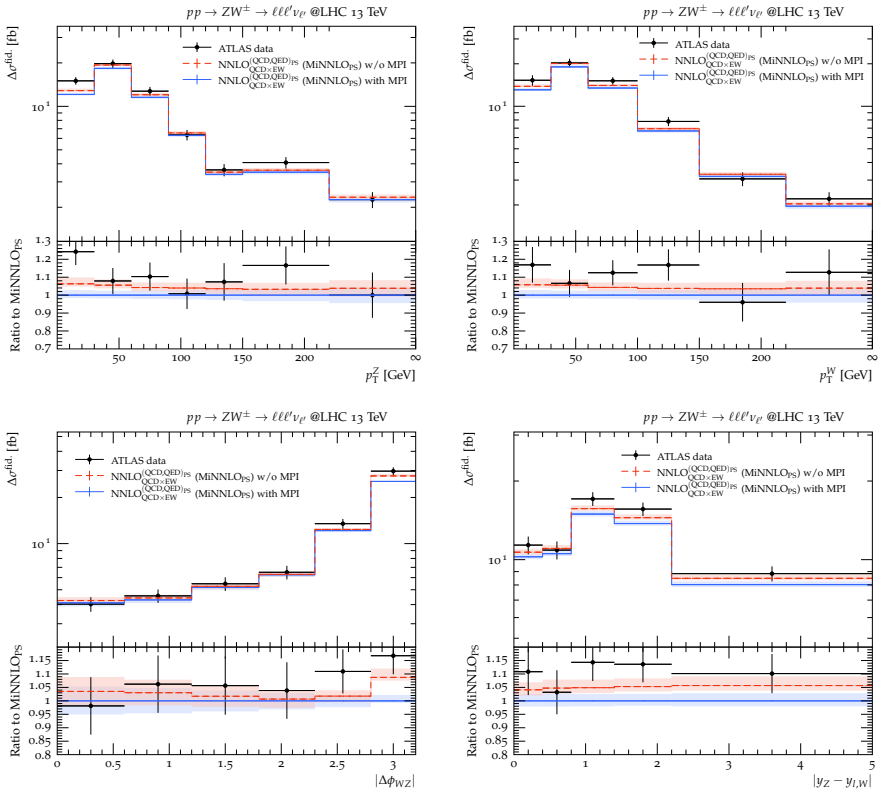

Figure 5: Comparison of our default prediction NNLO$^{(QCD,QED)_{PS}}_{QCDxEW}$ with (blue) and without (red) MPI effects with ATLAS data [36].

corresponds to leptons at large rapidities, for which not all the Mandelstam invariant $\hat{s}_{ij}$ are large. Double EW Sudakov logarithms, which are of the form $\ln^2(|\hat{s}_{ij}|/M_W^2)$, are thus suppressed. When we apply fiducial cuts, these very forward regions are excluded, leading to the typical EW enhancement in the tail of the $m_{3\ell}$ distribution. Notice that this observable is not affected by giant K-factors. More results are presented and discussed in the original publication [1].

We now present a comparison with recent ATLAS data [36] using as nominal prediction the multiplicative scheme with both QCD and QED parton showers switched on (NNLO$^{(QCD,QED)_{PS}}_{QCD\times EW}$). The comparison has been performed using the RIVET routines [37] provided on the `HEPdata` webpage https://www.hepdata.net/record/ins1720438. The following results (figure 5) show the differential cross section for $W^{\pm}Z$ production averaged over all combinations of electrons and muons in the final state. We present the transverse momenta of the Z boson ($p_{T,Z}$) and of the W boson ($p_{T,W}$), the opening azimuthal angle between the Z and the W bosons ($\Delta\phi_{WZ}$) and the absolute rapidity difference between the Z boson and the charged lepton coming from the W decay ($|y_Z - y_{\ell_W}|$). We present results with (blue curve) and without (red curve) multi-particle interactions (MPI). Our predictions are in good agreement with data, both in the bulk region of the cross section, where NNLO QCD computations are crucial, and in the tails of distributions, where EW effects have a non-negligible impact. Notice that the inclusion of MPI effects results in a shift of -5% of the distributions. Note that theoretical calculations are extremely precise when

compared to current data.

4. Conclusions

In this work we presented results for $W^{\pm}Z$ production at NNLO QCD and NLO EW accuracy consistently matched to parton showers. The combination of QCD and EW corrections is done through an a-posteriori reweighting. We presented a phenomenological analysis for 13 TeV LHC collisions, showing that NNLO QCD corrections matched to parton showers already provide a good description of the bulk of the cross section, while the inclusion of NLO EW effects becomes crucial for a correct description of the tails of distributions. Our results are in remarkable agreement with experimental data [36]: even though current data present large error bars due to statistical uncertainties, we expect our MiNNLO$_{\rm PS}$ generator to become a useful tool in the future for high-precision studies for $W^{\pm}Z$ production.

References

[1] J. M. Lindert, D. Lombardi, M. Wiesemann, G. Zanderighi and S. Zanoli, *WZ production at NNLO QCD and NLO EW matched to parton showers with MiNNLO$_{PS}$*, *JHEP* **11** (2022) 036, [2208.12660].

[2] M. Grazzini, S. Kallweit, D. Rathlev and M. Wiesemann, *$W^{\pm}Z$ production at hadron colliders in NNLO QCD*, *Phys. Lett.* **B761** (2016) 179–183, [1604.08576].

[3] R. W. Brown, D. Sahdev and K. O. Mikaelian, *W+- Z0 and W+- gamma Pair Production in Neutrino e, p p, and anti-p p Collisions*, *Phys. Rev. D* **20** (1979) 1164.

[4] T. Ježo and P. Nason, *On the Treatment of Resonances in Next-to-Leading Order Calculations Matched to a Parton Shower*, *JHEP* **12** (2015) 065, [1509.09071].

[5] T. Sjöstrand, S. Ask, J. R. Christiansen, R. Corke, N. Desai, P. Ilten, S. Mrenna, S. Prestel, C. O. Rasmussen and P. Z. Skands, *An Introduction to PYTHIA 8.2*, *Comput. Phys. Commun.* **191** (2015) 159–177, [1410.3012].

[6] P. F. Monni, P. Nason, E. Re, M. Wiesemann and G. Zanderighi, *MiNNLO$_{PS}$: A new method to match NNLO QCD to parton showers*, *JHEP* **05** (2020) 143, [1908.06987].

[7] P. F. Monni, E. Re and M. Wiesemann, *MiNNLO$_{PS}$: optimizing $2 \to 1$ hadronic processes*, *Eur. Phys. J. C* **80** (2020) 1075, [2006.04133].

[8] P. Nason, *A New method for combining NLO QCD with shower Monte Carlo algorithms*, *JHEP* **11** (2004) 040, [hep-ph/0409146].

[9] P. Nason and G. Ridolfi, *A Positive-weight next-to-leading-order Monte Carlo for Z pair hadroproduction*, *JHEP* **08** (2006) 077, [hep-ph/0606275].

[10] S. Frixione, P. Nason and C. Oleari, *Matching NLO QCD computations with Parton Shower simulations: the POWHEG method*, *JHEP* **11** (2007) 070, [0709.2092].

[11] S. Alioli, P. Nason, C. Oleari and E. Re, *A general framework for implementing NLO calculations in shower Monte Carlo programs: the POWHEG BOX*, *JHEP* **06** (2010) 043, [1002.2581].

[12] F. Cascioli, P. Maierhöfer and S. Pozzorini, *Scattering Amplitudes with Open Loops*, *Phys. Rev. Lett.* **108** (2012) 111601, [1111.5206].

[13] F. Buccioni, S. Pozzorini and M. Zoller, *On-the-fly reduction of open loops*, *Eur. Phys. J.* **C78** (2018) 70, [1710.11452].

[14] F. Buccioni, J.-N. Lang, J. M. Lindert, P. Maierhöfer, S. Pozzorini, H. Zhang and M. F. Zoller, *OpenLoops 2*, *Eur. Phys. J. C* **79** (2019) 866, [1907.13071].

[15] T. Ježo, J. M. Lindert, P. Nason, C. Oleari and S. Pozzorini, *An NLO+PS generator for $t\bar{t}$ and Wt production and decay including non-resonant and interference effects*, *Eur. Phys. J. C* **76** (2016) 691, [1607.04538].

[16] T. Gehrmann, A. von Manteuffel and L. Tancredi, *The two-loop helicity amplitudes for $q\bar{q}' \to V_1V_2 \to 4$ leptons*, *JHEP* **09** (2015) 128, [1503.04812].

[17] *The VVamp project, by T. Gehrmann, A. von Manteuffel, and L. Tancredi, is publicly available*, http://vvamp.hepforge.org.

[18] M. Grazzini, S. Kallweit and M. Wiesemann, *Fully differential NNLO computations with MATRIX*, *Eur. Phys. J.* **C78** (2018) 537, [1711.06631].

[19] D. Lombardi, M. Wiesemann and G. Zanderighi, *Advancing MiNNLO$_{PS}$ to diboson processes: $Z\gamma$ production at NNLO+PS*, *JHEP* **06** (2021) 095, [2010.10478].

[20] G. P. Salam and J. Rojo, *A Higher Order Perturbative Parton Evolution Toolkit (HOPPET)*, *Comput. Phys. Commun.* **180** (2009) 120–156, [0804.3755].

[21] A. Buckley, J. Ferrando, S. Lloyd, K. Nordström, B. Page, M. Rüfenacht, M. Schönherr and G. Watt, *LHAPDF6: parton density access in the LHC precision era*, *Eur. Phys. J.* **C75** (2015) 132, [1412.7420].

[22] T. Gehrmann and E. Remiddi, *Numerical evaluation of harmonic polylogarithms*, *Comput. Phys. Commun.* **141** (2001) 296–312, [hep-ph/0107173].

[23] M. Chiesa, C. Oleari and E. Re, *NLO QCD+NLO EW corrections to diboson production matched to parton shower*, *Eur. Phys. J. C* **80** (2020) 849, [2005.12146].

[24] F. Granata, J. M. Lindert, C. Oleari and S. Pozzorini, *NLO QCD+EW predictions for HV and HV +jet production including parton-shower effects*, *JHEP* **09** (2017) 012, [1706.03522].

[25] M. Grazzini, S. Kallweit, J. M. Lindert, S. Pozzorini and M. Wiesemann, *NNLO QCD + NLO EW with Matrix+OpenLoops: precise predictions for vector-boson pair production*, *JHEP* **02** (2020) 087, [1912.00068].

[26] Particle Data Group collaboration, P. A. Zyla et al., *Review of Particle Physics*, *PTEP* **2020** (2020) 083C01.

[27] A. Denner, S. Dittmaier, M. Roth and D. Wackeroth, *Predictions for all processes e+ e- —> 4 fermions + gamma*, *Nucl. Phys. B* **560** (1999) 33–65, [hep-ph/9904472].

[28] A. Denner, S. Dittmaier, M. Roth and L. H. Wieders, *Electroweak corrections to charged-current $e^+e^- \to 4$ fermion processes: Technical details and further results*, *Nucl. Phys.* **B724** (2005) 247–294, [hep-ph/0505042].

[29] A. Manohar, P. Nason, G. P. Salam and G. Zanderighi, *How bright is the proton? A precise determination of the photon parton distribution function*, *Phys. Rev. Lett.* **117** (2016) 242002, [1607.04266].

[30] A. V. Manohar, P. Nason, G. P. Salam and G. Zanderighi, *The Photon Content of the Proton*, *JHEP* **12** (2017) 046, [1708.01256].

[31] NNPDF collaboration, V. Bertone, S. Carrazza, N. P. Hartland and J. Rojo, *Illuminating the photon content of the proton within a global PDF analysis*, *SciPost Phys.* **5** (2018) 008, [1712.07053].

[32] P. Skands, S. Carrazza and J. Rojo, *Tuning PYTHIA 8.1: the Monash 2013 Tune*, *Eur. Phys. J. C* **74** (2014) 3024, [1404.5630].

[33] C. M. Carloni Calame, G. Montagna, O. Nicrosini and A. Vicini, *Precision electroweak calculation of the production of a high transverse-momentum lepton pair at hadron colliders*, *JHEP* **10** (2007) 109, [0710.1722].

[34] S. Dittmaier and M. Huber, *Radiative corrections to the neutral-current Drell-Yan process in the Standard Model and its minimal supersymmetric extension*, *JHEP* **01** (2010) 060, [0911.2329].

[35] S. Kallweit, J. M. Lindert, P. Maierhöfer, S. Pozzorini and M. Schönherr, *NLO QCD+EW predictions for V + jets including off-shell vector-boson decays and multijet merging*, *JHEP* **04** (2016) 021, [1511.08692].

[36] ATLAS collaboration, M. Aaboud et al., *Measurement of $W^{\pm}Z$ production cross sections and gauge boson polarisation in pp collisions at $\sqrt{s} = 13$ TeV with the ATLAS detector*, *Eur. Phys. J. C* **79** (2019) 535, [1902.05759].

[37] C. Bierlich et al., *Robust Independent Validation of Experiment and Theory: Rivet version 3*, *SciPost Phys.* **8** (2020) 026, [1912.05451].